ACS OMEGA

http://pubs.acs.org/journal/acsodf

Article

Femtosecond Laser Micromachining of the Mask for Acoustofluidic Device Preparation

Yong Wang and Jingui Qian*

Cite This: *ACS Omega* 2023, 8, 7838−7844

Read Online

ACCESS | Metrics & More | Article Recommendations

ABSTRACT: Surface acoustic wave (SAW)-based acoustofluidic devices have shown broad applications in microfluidic actuation and particle/cell manipulation. Conventional SAW acoustofluidic device fabrication generally includes photolithography and lift-off processes and thus requires accessing cleanroom facilities and expensive lithography equipment. In this paper, we report a femtosecond laser direct writing mask method for acoustofluidic device preparation. By micromachining of steel foil to form the mask and direct evaporation of metal on the piezoelectric substrate using the mask, the interdigital transducer (IDT) electrodes of the SAW device are generated. The minimum spatial periodicity of the IDT finger is about 200 μm, and the preparation for $LiNbO_3$ and ZnO thin films and flexible PVDF SAW devices is verified. Meanwhile, we have demonstrated various microfluidic functions, including streaming, concentration, pumping, jumping, jetting, nebulization, and particle alignment using the fabricated acoustofluidic (ZnO/Al plate, $LiNbO_3$) devices. Compared to the traditional manufacturing process, the proposed method omits spin coating, drying, lithography, developing, and lift-off processes and thus has advantages of simple, convenient, low cost, and environment friendliness.

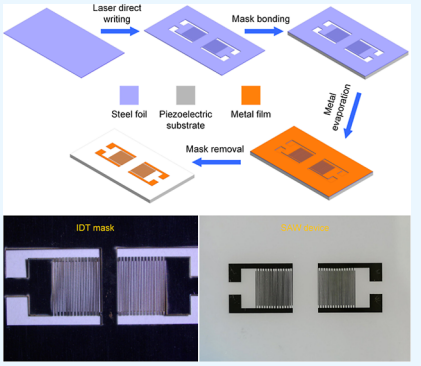

1. INTRODUCTION

Efficient actuation of fluids and dexterous handling of micro-objects on the micro-/nanoscale are critical to microfluidic lab-on-a-chip systems.[1−3] Applications of surface acoustic waves (SAWs) in microfluidic platforms (often called as acoustofluidics) have recently gained great interest for manipulating fluids, microparticles/cells, in either a digital form (sessile droplet) or a continuous flow (inside a channel/chamber).[4−8] These acoustofluidic devices have shown remarkable potential in mixing,[9,10] pumping,[11] jetting,[12,13] and atomizing[14,15] of fluids on the microscale and applications in the fields of biomedicine and chemistry for non-invasive and contactless manipulation, with low cost, good biocompatibility, and conserved cell viability and proliferation capacity.[16−20] SAW acoustofluidic devices are generally fabricated by pattering IDTs on a piezoelectric substrate such as a $LiNbO_3$ or a piezoelectric film on a silicon or Al plate substrate,[21−23] which converts the radio frequency (RF) signal into SAWs propagating along the surface of the substrate. When the SAW meets a liquid medium, it changes the wave mode to a leaky SAW and dissipates acoustic energy into liquid through viscous damping,[24,25] inducing acoustic streaming in fluids and imparting an acoustic radiation force to the suspended particles/cells in liquids.[26−28]

To obtain IDT electrodes, conventional SAW devices are generally manufactured through photolithography and lift-off processes. These methods can provide a high machining precision to the nanometer scale and make it easy to fabricate high-frequency SAW devices above GHz.[29,30] However, they also involve the following steps done in cleanroom: spin-coating, heating, lithography, developing, evaporation, lift-off, and so forth. These manufacturing processes not only require an expensive lithography machine and a clean environment but also produce a large amount of chemical waste liquid to deal with.[31,32] What is more, large amounts of used chemicals and other consumables are also the cost-effectiveness of manufacturing. However, for most SAW acoustofluidic devices, they often operate at a low frequency (about 10−20 MHz),[33−36] with a large wavelength up to hundreds of micrometers, as a large wavelength or low frequency can improve the SAW penetration depth in fluids,[37,38] thereby enhancing the driving efficiency. Therefore, the machining accuracy requirement for SAW acoustofluidic devices is not high. Recently, some alternative techniques for making IDT electrodes of SAW acoustofluidic devices have been reported. Rezk et al. reported a stacking aluminum foil strip onto the $LiNbO_3$ substrate method for acoustofluidic device fabrication.[39] However, the size of aluminum foil strips reaches several millimeters, and the

Received: November 28, 2022
Accepted: February 3, 2023
Published: February 14, 2023

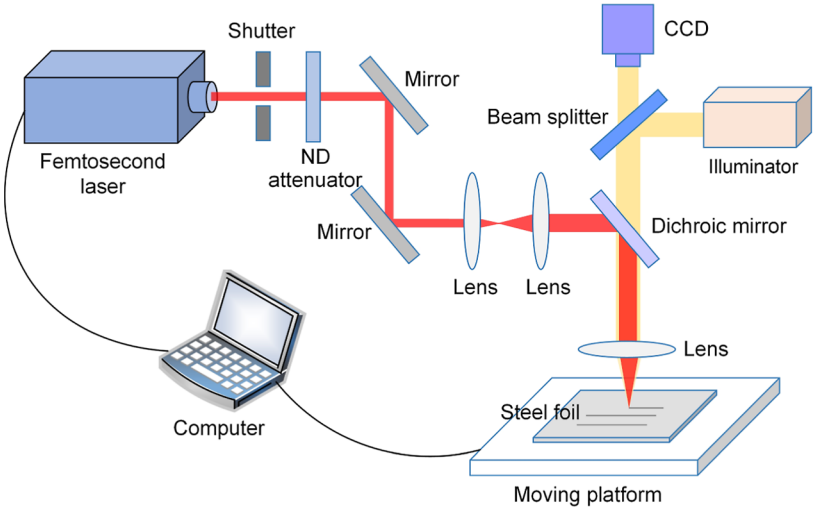

Figure 1. Schematic of the experimental setup for femtosecond laser micromachining of the steel foil-based IDT mask.

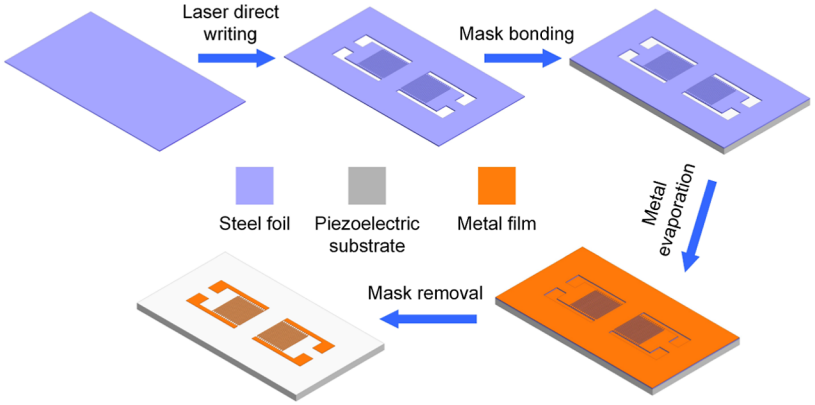

Figure 2. Fabrication processes for IDT electrodes of the SAW acoustofluidic device using the femtosecond laser direct writing mask method.

excited acoustic wave is Lamb wave with the frequency of MHz order. IDTs have also been created by pouring a low-melting point metal into an IDT mold made by the PDMS.[40] However, the electrode channel fabrication requires the lithography process, and the device may be invalid in a high-temperature environment. A more accurate manufacturing technique was achieved by clamping a printed circuit board (PCB) with an IDT electrode pattern onto a $LiNbO_3$ substrate to make acoustofluidic devices.[32,41,42] However, the contact between the IDT electrodes and the substrate may be a problem, thereby achieving a lower electromechanical coupling efficiency. Therefore, there is an increasing demand for a low-cost, convenient, reliable, and experimental friendly method for acoustofluidic device preparation.

Femtosecond laser micromachining technologies have been demonstrated as a promising solution for high-precision and flexible fabrication of planar or three-dimensional (3D) microstructures, such as optical waveguides,[43] microfluidic chips,[44] microchannels,[45] and microelectrode arrays.[46] In comparison with picosecond and nanosecond lasers, the femtosecond laser has a higher peak power, thereby significantly reducing the edge heat-affected zone and the kerf width and improving the machining precision. In addition, the programmable 3D processing capability, high spatial resolution, and smaller thermal ablation make the femtosecond laser a promising enabler for low-cost, high-precision, and personalized micromachining of a thin-film IDT mask.[47−49] When the metal film is evaporated on a piezoelectric substrate using the IDT mask, the IDT electrode is then generated. Compared to conventional photolithography and lift-off processes, the manufacturing process can be significantly simplified and avoids the use of the expensive photoresist, chemical waste disposal, and the requirement for cleanroom facilities. Moreover, as the preparation process omits the drying for the photoresist (generally >100 °C), it is more suitable for the fabrication of IDT electrodes on the piezoelectric substrate that is not heat-resisting. However, whether the fabricated SAW device can meet the requirement for acoustofluidic functions needs to be further investigated.

In this paper, we report a femtosecond laser direct writing mask method for IDT electrode preparation of SAW devices and investigate their acoustofluidic functions. We have achieved a minimum spatial periodicity of ∼200 μm for the IDT mask (an electrode width of ∼50 μm), and the fabrication for $LiNbO_3$ and ZnO thin films and PVDF SAW devices is verified. Moreover, various microfluidic functions, including streaming, concentration, pumping, jumping, jetting, nebulization, and particle arrangement, have been demonstrated using the fabricated SAW devices. The proposed method has the advantages of low cost, simplicity, and environment friendliness. Furthermore, as the steel foil mask is of low cost, flexible, and reusable, it can be further used to prepare the

https://doi.org/10.1021/acsomega.2c07589
ACS Omega 2023, 8, 7838−7844

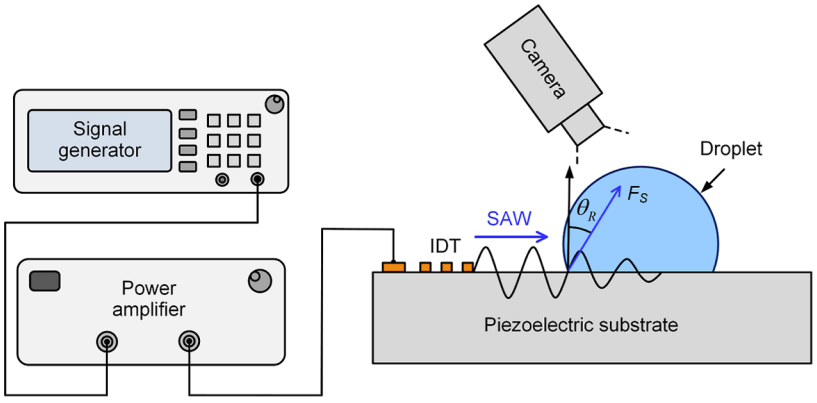

Figure 3. Schematic of the experimental setup for the microfluidic actuation experiment. Here, F_S is the SAW driving force and θ_R is the Rayleigh angle.

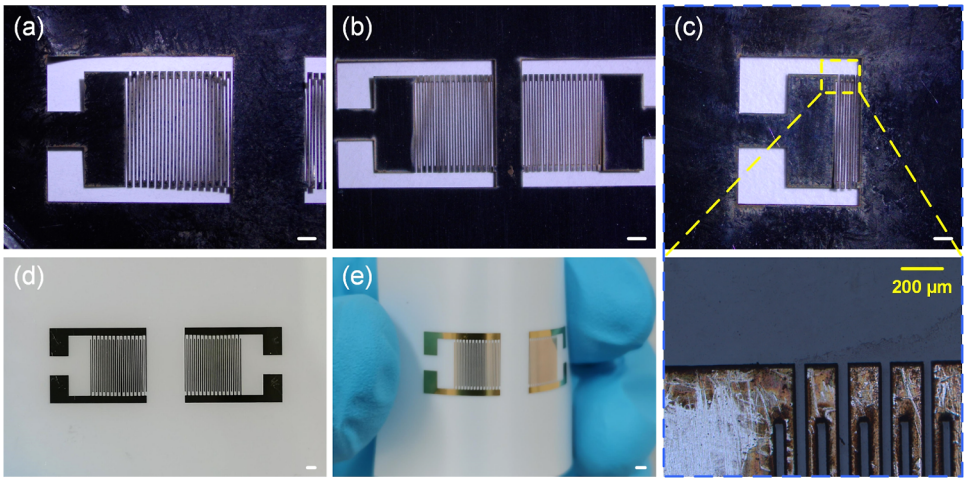

Figure 4. Optical images of the IDT masks with wavelengths of (a) 400, (b) 300, and (c) 200 μm. Optical images of the SAW devices fabricated on the (d) $LiNbO_3$ substrate (500 μm thick) and (e) PVDF substrate (200 μm thick). All scale bars are 1 mm.

metal pattern on the curved surface and extends the applications to flexible electronics and industrial production.

2. EXPERIMENTAL SECTION

2.1. IDT Mask Micromachining. The schematic of a femtosecond laser micromachining system for IDT mask preparation is shown in Figure 1. A diode-pumped ultrafast fiber femtosecond laser (Amplitude) delivering a central wavelength of 1030 nm, a pulse duration of 130 fs, and a beam diameter of 3 mm (at e^{-2}) was used. Then, the laser beam diameter was expanded to 9 mm by a beam expander. Finally, the expanded laser beam was focused onto the steel foil with a thickness of 10 μm through a lens (focal length f = 20 mm). The steel foil was put on a three-dimensional moving platform to realize IDT pattern micromachining. In addition, a CCD camera was used for real-time observation of the machining process. The laser machining power can be adjusted by the pulse repetition rate and a neutral density (ND) attenuator. During the micromachining process, the repetition rate of the femtosecond laser is set as 2 kHz, with a power of 80−100 mW, and the scanning speed of the moving platform is about 0.25−0.35 mm/s. When the cutting speed is set as 0.3 mm/s, the fabrication time for an IDT (20 pairs of fingers and an acoustic aperture of 5 mm) is about 30 min.

2.2. SAW Device Fabrication. Figure 2 shows the fabrication processes for IDT electrodes of the SAW device. First, the IDT mask was generated using femtosecond laser micromachining of the commercially available steel foil with a thickness of 10 μm. Then, the IDT mask was fixed onto the piezoelectric substrate using conductive tapes. For the $LiNbO_3$ piezoelectric substrate, the IDT mask needs to be aligned due to its anisotropic piezoelectric property. After that, the bonded IDT mask and the piezoelectric substrate were put into a high-vacuum evaporation coating system to form the metal film [Cr (5 nm)/Au (100 nm)]. Finally, the IDT electrodes were generated by removing the mask from the surface of the piezoelectric substrate.

2.3. Acoustofluidic Testing. The schematic of the experimental setup for the microfluidic test is shown in Figure 3. The RF signal was generated using a signal generator (RIGOL, DG4162) and amplified by a power amplifier (Aigtek, ATA-1222A); then, the amplified signal was fed into the IDT of the SAW device for microfluidic actuation or particle manipulation. The input SAW power was measured using a RF power meter (DIAMOND, SX200). To reduce the motion resistance of the droplet, the surface of the SAW device was treated with a layer of ∼200 nm-thick fluoropolymer coating (CYTOP, Asahi Glass Co., Tokyo, Japan) and heated to 120 °C for 10 min to make the surface hydrophobic, whereas for the nebulization test, the surface needed to be treated as hydrophilic. For the particle arrangement experiment, a PDMS chamber fabricated by the soft photo-

https://doi.org/10.1021/acsomega.2c07589
ACS Omega 2023, 8, 7838−7844

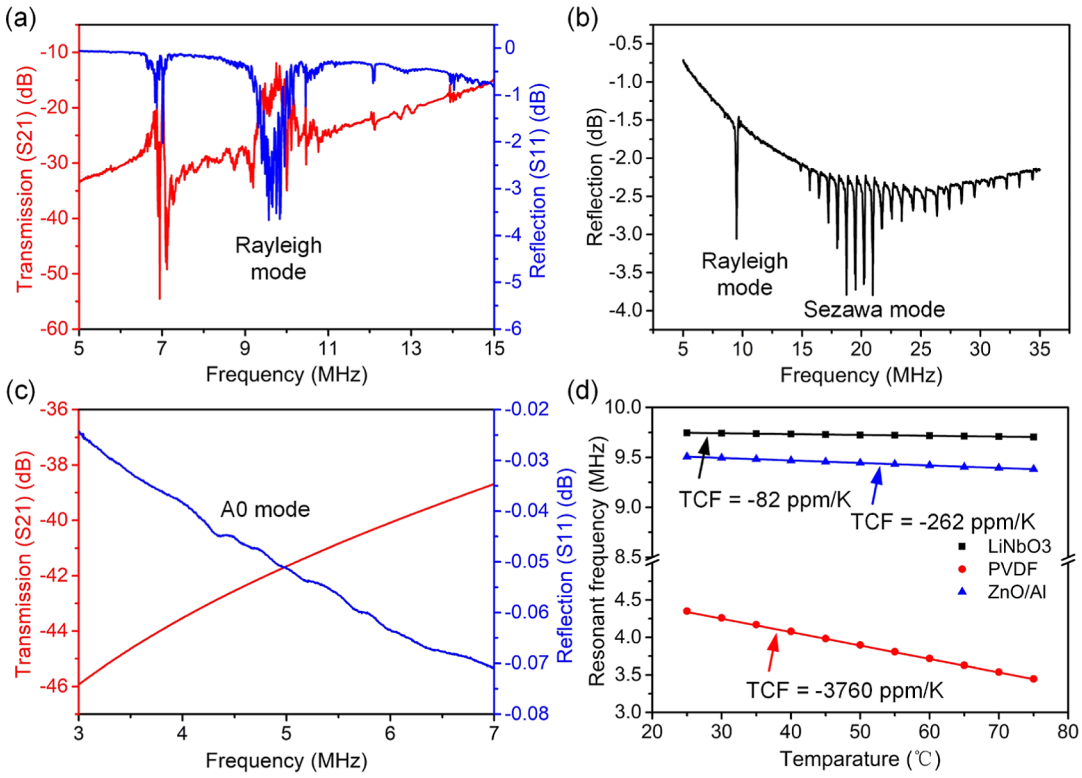

Figure 5. Signal transmission and reflection spectra for the (a) $LiNbO_3$ SAW device, (b) ZnO/Al plate SAW device, and (c) PVDF SAW device. (d) Resonant frequency changes as a function of temperature for different substrate SAW devices.

lithography process was bonded onto the SAW device surface.[22] The suspended polystyrene microspheres with a diameter of 10 μm were used for the particle arrangement experiment in liquid. Meanwhile, a high-speed video camera (NPX-GS130UM, 200 frames/s) was used to observe acoustofluidic behaviors.

3. RESULTS AND DISCUSSION

3.1. Device Characterization. Figure 4a–c shows the fabricated steel foil-based IDT mask with wavelengths of 200–400 μm using the femtosecond laser micromachining method. As the steel foil substrate is flexible, the minimum spatial periodicity of the IDT finger is about 200 μm; otherwise, the cut IDT electrode will be difficult to remove from the steel foil substrate. In addition, although a smaller focal length objective lens can decrease the kerf width and improve the machining resolution, the thermal deformation of the steel foil substrate during the machining will result in defocus of the light spot and thus causes incomplete cutting of the substrate for a smaller Rayleigh length of the objective lens. A thicker steel foil substrate can weaken the thermal deformation effect, whereas it needs multiple cutting of steel foil, thereby reducing the machining precision. The edge burr of the IDT mask is below 1 μm, meeting the requirement for acoustofluidic device preparation. Figure 4d,e shows the fabricated SAW device on the $LiNbO_3$ and PVDF substrate, indicating that the proposed method is suitable for the preparation of various piezoelectric substrate-based SAW devices.

The resonant characteristics of the fabricated SAW devices were then characterized using a network analyzer (Agilent E5061B), with reflection and transmission spectra shown in Figure 5a–c. Here, the wavelength of the $LiNbO_3$ and PVDF SAW devices is 400 μm, and the wavelength of the ZnO/Al plate (1.5 mm thick) SAW device is 300 μm. The $LiNbO_3$ SAW device shows an apparent resonant peak at ∼9.75 MHz (Rayleigh mode), corresponding to an acoustic wave speed of ∼3900 m/s, which coincides with the results reported in previous studies.[37,50] For the ZnO thin-film (5 μm)-based Al plate (1.5 mm-thick) SAW device, the acoustic speed of the ZnO film (2700 m/s) is smaller than that of the Al substrate (∼2900 m/s), thus generating both the Rayleigh mode and the Sezawa mode,[22] corresponding to resonant frequencies of 9.45 and 18.7 MHz, respectively. The Rayleigh wave speed of the ZnO/Al substrate (2835 m/s) is nearly the same as that of the Al plate, due to which the SAW device wavelength (300 μm) is much larger than the thickness (5 μm) of the ZnO film, which results in more acoustic waves propagating in the Al plate substrate. For the PVDF SAW device, only a weak reflection peak (corresponding to the A0 mode with a resonant frequency of 4.33 MHz) was observed, and there is no apparent transmission due to significant acoustic energy dissipation into PVDF the substrate. Therefore, the PVDF-based SAW device is not suitable for acoustofluidic applications. Figure 5d shows resonant frequency changes of the SAW devices as a function of temperature. The measured temperature coefficient of frequency (TCF) for $LiNbO_3$, ZnO/Al plate, and PVDF SAW devices is −82, −262, and −3760 ppm/K, respectively. Although the PVDF-based SAW device presents a higher TCF, the piezoelectric property of PVDF is weakened at a temperature above 100 °C and thus is not suitable for high-temperature sensing applications, whereas for the ZnO/Al plate SAW device, ZnO can maintain a good piezoelectric property up to 400 °C[50] and therefore can be used as a high-temperature sensor, such as a temperature-based gas flow rate sensor.[51]

https://doi.org/10.1021/acsomega.2c07589
ACS Omega 2023, 8, 7838−7844

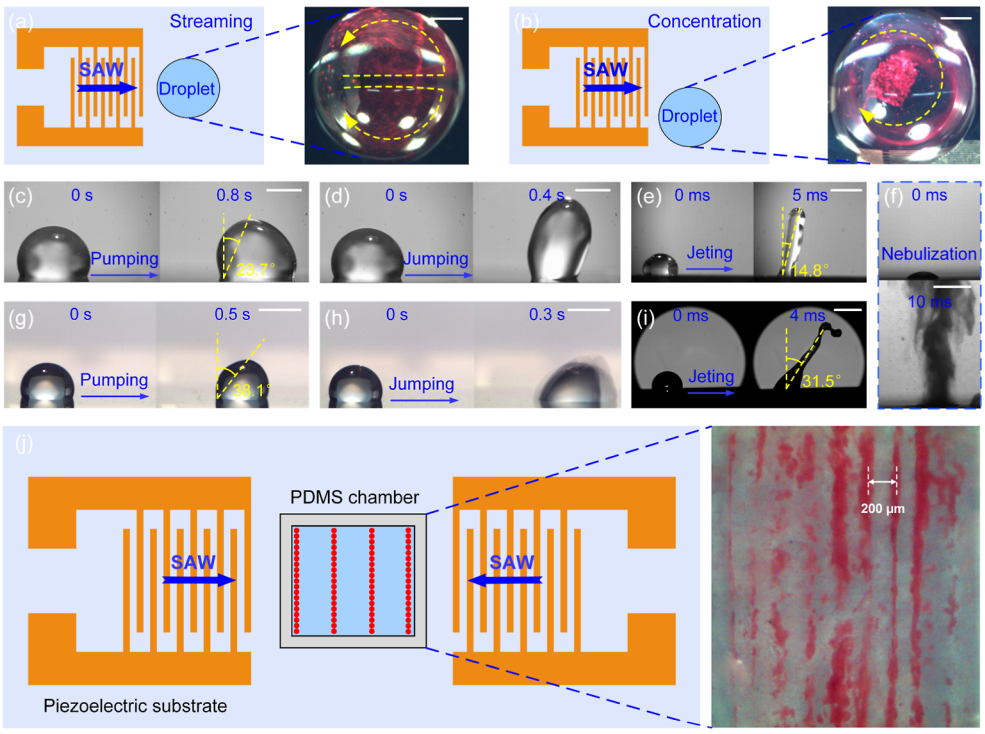

Figure 6. (a) Acoustic streaming pattern when the liquid droplet with suspended particles is placed in the center of the acoustic aperture and (b) acoustic concentration of particles when the liquid droplet with suspended particles is positioned off the central line of the acoustic aperture. Liquid droplet (c) pumping, (d) jumping, (e) jetting, and (f) nebulization using the $LiNbO_3$ SAW device with an applied power of 0.6, 1.2, 1.6, and 2.5 W, respectively. Liquid droplet (g) pumping, (h) jumping, and (i) jetting using the ZnO/Al plate SAW device with an applied power of 1.5, 8, and 14 W, respectively. (j) Particle arrangement in a PDMS microchamber using the $LiNbO_3$ SAW device. All scale bars are 1 mm.

3.2. Demonstration of Acoustofluidic Functions.

Then, we further investigated acoustofluidic functions using the fabricated $LiNbO_3$ and ZnO/Al plate SAW devices. When a liquid droplet is located on the SAW propagation path, the SAW interacts with the liquid and the acoustic energy couples into the liquid, inducing the acoustic streaming pattern.[37] These patterns can be observed if microscale particles are dispersed into the liquid. Figure 6a,b demonstrates acoustic streaming and particle concentration phenomena in the liquid droplet using the fabricated ZnO/Al plate SAW device. When a liquid droplet with suspended particles was placed in the center of the acoustic aperture of the SAW device, a typical butterfly pattern with a double vortex was generated after applying an RF power of 0.1 W, whereas particle concentration phenomena would be observed if a liquid droplet with suspended particles was positioned off the central line of the acoustic aperture due to the asymmetric acoustic streaming force and its causing vortex flow.

With the increase of applied power, the liquid droplet pumping, jumping, and jetting were then achieved using the fabricated $LiNbO_3$ and ZnO/Al plate SAW device, respectively, as shown in Figure 6c−e,g−i. The droplet lateral deformation and jetting angle driven by the $LiNbO_3$ SAW device are smaller than those of the ZnO/Al plate SAW device, due to which the acoustic speed of the $LiNbO_3$ substrate (3900 m/s) is larger than that of the ZnO/Al plate substrate (~2800 m/s), which generates a smaller Rayleigh angle ($\theta_R = \sin^{-1}(C_F/C_S)$, where C_F is the sound speed in the liquid and C_S is the SAW propagation speed in the substrate). As the SAW driving force direction is along the Rayleigh angle, a smaller Rayleigh angle will result in a smaller lateral deformation and jetting angle of the droplet. The measured droplet jetting angle for $LiNbO_3$ and ZnO/Al plate SAW devices is 14.8 and 31.5°, respectively, nearly along the Rayleigh angle of the SAW device (~21° for the $LiNbO_3$ SAW device and ~31° for the ZnO/Al plate SAW device), which are in good agreements with the previous study.[12] When the input SAW power is further increased and the device surface is hydrophobic, liquid nebulization using the $LiNbO_3$ SAW device was then observed, as shown in Figure 6f. Moreover, as shown in Figure 6j, we have also achieved particle linear alignment in the PDMS microchamber (2 mm × 3 mm) using the $LiNbO_3$ SAW device with a wavelength of 400 μm, demonstrating the acoustic tweezer function. The distance between adjacent traces is about 200 μm, corresponding to the half-wavelength ($\lambda_{SAW}/2$) of the SAW device, which is consistent with the previous study.[28]

4. CONCLUSIONS

In summary, a femtosecond laser direct writing mask method has been proposed for acoustofluidic device preparation. The IDT electrodes of SAW acoustofluidic devices are fabricated by direct evaporation of a metal film on the piezoelectric substrate using the steel foil-based IDT mask with a thickness of 10 μm. The preparation of the SAW device on the $LiNbO_3$ substrate, the ZnO thin-film on the Al plate substrate, and the PVDF substrate has been verified with a minimum IDT finger width of 50 μm (wavelength 200 μm), and the resonant characteristics and TCF of these devices were characterized. Based on the fabricated $LiNbO_3$ and ZnO/Al plate SAW devices, we have demonstrated various microfluidic functions, including streaming, concentration, pumping, jumping, jetting, nebulization, and particle alignment, indicating a good acoustofluidic function using these fabricated devices. In comparison

https://doi.org/10.1021/acsomega.2c07589
ACS Omega 2023, 8, 7838−7844

with conventional photolithography and lift-off manufacturing processes, the proposed method has advantages of simplicity, low cost, suitability for customization, and environment friendliness.

AUTHOR INFORMATION

Corresponding Author

Jingui Qian − *Anhui Province Key Laboratory of Measuring Theory and Precision Instrument, School of Instrument Science and Opto-Electronics Engineering, Hefei University of Technology, Hefei 230009, China*; Email: jgqian@hfut.edu.cn

Author

Yong Wang − *Department of Mechanical Engineering, Hangzhou City University, Hangzhou 310015, China; The State Key Laboratory of Fluid Power and Mechatronic Systems, Zhejiang University, Hangzhou 310027, China*; orcid.org/0000-0002-4397-1670

Complete contact information is available at: https://pubs.acs.org/10.1021/acsomega.2c07589

Notes

The authors declare no competing financial interest.

ACKNOWLEDGMENTS

This work was supported by the "National Natural Science Foundation of China (62005226)" and the Open Foundation of the State Key Laboratory of Fluid Power and Mechatronic Systems. The authors thank the technical support from the Center for Micro/Nano Fabrication and Instrumentation at Westlake University.

REFERENCES

(1) Destgeer, G.; Sung, H. J. Recent advances in microfluidic actuation and micro-object manipulation via surface acoustic waves. *Lab Chip* **2015**, *15*, 2722−2738.

(2) Ding, X.; Lin, S. C. S.; Kiraly, B.; Yue, H.; Li, S.; Chiang, I. K.; Shi, J.; Benkovic, S. J.; Huang, T. J. On-chip manipulation of single microparticles, cells, and organisms using surface acoustic waves. *Proc. Natl. Acad. Sci. U.S.A.* **2012**, *109*, 11105−11109.

(3) Tao, R.; McHale, G.; Reboud, J.; Cooper, J. M.; Torun, H.; Luo, J.; Luo, J.; Yang, X.; Zhou, J.; Canyelles-Pericas, P.; Wu, Q.; Fu, Y. Hierarchical nanotexturing enables acoustofluidics on slippery yet sticky, flexible surfaces. *Nano Lett.* **2020**, *20*, 3263−3270.

(4) Maramizonouz, S.; Tao, X.; Rahmati, M.; Jia, C.; Tao, R.; Torun, H.; Zheng, T.; Jin, H.; Dong, S.; Luo, J.; Fu, Y. Flexible and bendable acoustofluidics for particle and cell patterning. *Int. J. Mech. Sci.* **2021**, *202*−*203*, 106536.

(5) Li, P.; Huang, T. J. Applications of acoustofluidics in bioanalytical chemistry. *Anal. Chem.* **2018**, *91*, 757−767.

(6) Yang, S.; Tian, Z.; Wang, Z.; Rufo, J.; Li, P.; Mai, J.; Xia, J.; Bachman, H.; Huang, P. H.; Wu, M.; Chen, C.; Lee, L. P.; Huang, T. J. Harmonic acoustics for dynamic and selective particle manipulation. *Nat. Mater.* **2022**, *21*, 540−546.

(7) Wang, Y.; Zhang, Q.; Tao, R.; Xie, J.; Canyelles-Pericas, P.; Torun, H.; Reboud, J.; McHale, G.; Dodd, L. E.; Yang, X.; Luo, J.; Wu, Q.; Fu, Y. Flexible/bendable acoustofluidics based on thin-film surface acoustic waves on thin aluminum sheets. *ACS Appl. Mater. Interfaces* **2021**, *13*, 16978−16986.

(8) Friend, J.; Yeo, L. Y. Microscale acoustofluidics: microfluidics driven via acoustics and ultrasonics. *Rev. Mod. Phys.* **2011**, *83*, 647.

(9) Chen, Z.; Shen, L.; Zhao, X.; Chen, H.; Xiao, Y.; Zhang, Y.; Yang, X.; Zhang, J.; Wei, J.; Hao, N. Acoustofluidic micromixers: from rational design to lab-on-a-chip applications. *Appl. Mater. Today* **2022**, *26*, 101356.

(10) Chen, X.; Ning, Y.; Pan, S.; Liu, B.; Chang, Y.; Pang, W.; Duan, X. Mixing during trapping enabled a continuous-flow microfluidic smartphone immunoassay using acoustic streaming. *ACS Sens.* **2021**, *6*, 2386−2394.

(11) Wang, Y.; Tao, X.; Tao, R.; Zhou, J.; Zhang, Q.; Chen, D.; Jin, H.; Dong, S.; Xie, J.; Fu, Y. Q. Acoustofluidics along inclined surfaces based on AlN/Si Rayleigh surface acoustic waves. *Sens. Actuators A: Phys.* **2020**, *306*, 111967.

(12) Li, J.; Biroun, M. H.; Tao, R.; Wang, Y.; Torun, H.; Xu, N.; Rahmati, M.; Li, Y.; Gibson, D.; Fu, C.; Luo, J.; Dong, L.; Xie, J.; Fu, Y. Wide range of droplet jetting angles by thin-film based surface acoustic waves. *J. Physics D: Appl. Phys.* **2020**, *53*, 355402.

(13) Jangi, M.; Luo, J. T.; Tao, R.; Reboud, J.; Wilson, R.; Cooper, J. M.; Gibson, D.; Fu, Y. Q. Concentrated vertical jetting mechanism for isotropically focused ZnO/Si surface acoustic waves. *Int. J. Multiphase Flow* **2019**, *114*, 1−8.

(14) Roudini, M.; Niedermeier, D.; Stratmann, F.; Winkler, A. Droplet generation in standing-surface-acoustic-wave nebulization at controlled air humidity. *Phys. Rev. Appl.* **2020**, *14*, 014071.

(15) Sun, D.; Böhringer, K. F.; Sorensen, M.; Nilsson, E.; Edgar, J. S.; Goodlett, D. R. Droplet delivery and nebulization system using surface acoustic wave for mass spectrometry. *Lab Chip* **2020**, *20*, 3269−3277.

(16) Mutafopulos, K.; Spink, P.; Lofstrom, C. D.; Lu, P. J.; Lu, H.; Sharpe, J. C.; Franke, T.; Weitz, D. A. Traveling surface acoustic wave (TSAW) microfluidic fluorescence activated cell sorter (μFACS). *Lab Chip* **2019**, *19*, 2435−2443.

(17) Inui, T.; Mei, J.; Imashiro, C.; Kurashina, Y.; Friend, J.; Takemura, K. Focused surface acoustic wave locally removes cells from culture surface. *Lab Chip* **2021**, *21*, 1299−1306.

(18) Nam, H.; Sung, H. J.; Park, J.; Jeon, J. S. Manipulation of cancer cells in a sessile droplet via travelling surface acoustic waves. *Lab Chip* **2022**, *22*, 47−56.

(19) Chen, Z.; Pei, Z.; Zhao, X.; Zhang, J.; Wei, J.; Hao, N. Acoustic microreactors for chemical engineering. *Chem. Eng. J.* **2022**, *433*, 133258.

(20) Ning, S.; Liu, S.; Xiao, Y.; Zhang, G.; Cui, W.; Reed, M. A microfluidic chip with a serpentine channel enabling high-throughput cell separation using surface acoustic waves. *Lab Chip* **2021**, *21*, 4608−4617.

(21) He, X.; Chen, K.; Kong, L.; Li, P. Single-crystalline $LiNbO_3$ film based wideband SAW devices with spurious-free responses for future RF front-ends. *Appl. Phys. Lett.* **2022**, *120*, 113507.

(22) Wang, Y.; Zhang, Q.; Tao, R.; Chen, D.; Xie, J.; Torun, H.; Dodd, L. E.; Luo, J.; Fu, C.; Vernon, J.; Canyelles-Pericas, P.; Binns, R.; Fu, Y. A rapid and controllable acoustothermal microheater using thin film surface acoustic waves. *Sens. Actuators A: Phys.* **2021**, *318*, 112508.

(23) Yang, D.; Tao, R.; Hou, X.; Torun, H.; McHale, G.; Martin, J.; Fu, Y. Nanoscale "Earthquake" Effect Induced by Thin Film Surface Acoustic Waves as a New Strategy for Ice Protection. *Adv. Mater. Interfaces* **2021**, *8*, 2001776.

(24) Wang, Y.; Chen, D.; Wu, C.; Xie, J. Effect of droplet boundary behaviors on SAW attenuation for potential microfluidic applications. *Jpn J. Appl. Phys.* **2019**, *58*, 037001.

(25) Qi, Q. Attenuated leaky Rayleigh waves. *J. Acoust. Soc. Am.* **1994**, *95*, 3222−3231.

(26) Shiokawa, S.; Matsui, Y.; Moriizumi, T. Experimental study on liquid streaming by SAW. *Jpn J. Appl. Phys.* **1989**, *28*, 126.

(27) Destgeer, G.; Cho, H.; Ha, B. H.; Jung, J. H.; Park, J.; Sung, H. J. Acoustofluidic particle manipulation inside a sessile droplet: four distinct regimes of particle concentration. *Lab Chip* **2016**, *16*, 660−667.

(28) Tao, X.; Nguyen, T.; Jin, H.; Tao, R.; Luo, J.; Yang, X.; Torun, H.; Zhou, J.; Huang, S.; Shi, L.; Gibson, D.; Cooke, M. H.; Du, S.; Dong, J.; Luo, Y. Q.; Fu, Y. 3D patterning/manipulating micro-

particles and yeast cells using ZnO/Si thin film surface acoustic waves. *Sens. Actuators B: Chem.* **2019**, *299*, 126991.
(29) Zheng, J.; Zhou, J.; Zeng, P.; Liu, Y.; Shen, Y.; Yao, W.; Chen, Z.; Wu, J.; Xiong, S.; Chen, Y.; Shi, X.; Liu, J.; Fu, Y.; Duan, H. 30 GHz surface acoustic wave transducers with extremely high mass sensitivity. *Appl. Phys. Lett.* **2020**, *116*, 123502.
(30) Lamanna, L.; Rizzi, F.; Bhethanabotla, V. R.; De Vittorio, M. GHz AlN-based multiple mode SAW temperature sensor fabricated on PEN substrate. *Sens. Actuators A: Phys.* **2020**, *315*, 112268.
(31) Ding, X.; Peng, Z.; Lin, S. C. S.; Geri, M.; Li, S.; Li, P.; Chen, Y.; Dao, M.; Suresh, S.; Huang, T. J. Cell separation using tilted-angle standing surface acoustic waves. *Proc. Natl. Acad. Sci. U.S.A.* **2014**, *111*, 12992−12997.
(32) Sun, C.; Mikhaylov, R.; Fu, Y.; Wu, F.; Wang, H.; Yuan, X.; Xie, Z.; Liang, D.; Wu, Z.; Yang, X. Flexible printed circuit board as novel electrodes for acoustofluidic devices. *IEEE T. Electron Dev.* **2020**, *68*, 393−398.
(33) Tao, R.; Reboud, J.; Torun, H.; McHale, G.; Dodd, L. E.; Wu, Q.; Tao, K.; Yang, X.; Luo, J. T.; Todryk, S.; Fu, Y. Integrating microfluidics and biosensing on a single flexible acoustic device using hybrid modes. *Lab Chip* **2020**, *20*, 1002−1011.
(34) Shi, J.; Huang, H.; Stratton, Z.; Huang, Y.; Huang, T. J. Continuous particle separation in a microfluidic channel via standing surface acoustic waves (SSAW). *Lab Chip* **2009**, *9*, 3354−3359.
(35) Guo, F.; Mao, Z.; Chen, Y.; Xie, Z.; Lata, J. P.; Li, P.; Ren, L.; Liu, J.; Yang, J.; Dao, M.; Suresh, S.; Huang, T. J. Three-dimensional manipulation of single cells using surface acoustic waves. *Proc. Natl. Acad. Sci. U.S.A.* **2016**, *113*, 1522−1527.
(36) Qian, J.; Begum, H.; Lee, J. E. Y. Acoustofluidic localization of sparse particles on a piezoelectric resonant sensor for nanogram-scale mass measurements. *Microsyst. Nanoeng.* **2021**, *7*, 61.
(37) Guo, Y. J.; Lv, H. B.; Li, Y. F.; He, X. L.; Zhou, J.; Luo, J. K.; Zu, X. T.; Walton, A. J.; Fu, Y. Q. High frequency microfluidic performance of $LiNbO_3$ and ZnO surface acoustic wave devices. *J. Appl. Phys.* **2014**, *116*, 024501.
(38) Schmid, L.; Wixforth, A.; Weitz, D. A.; Franke, T. Novel surface acoustic wave (SAW)-driven closed PDMS flow chamber. *Microfluid. Nanofluid.* **2012**, *12*, 229−235.
(39) Rezk, A. R.; Friend, J. R.; Yeo, L. Y. Simple, low cost MHz-order acoustomicrofluidics using aluminium foil electrodes. *Lab Chip* **2014**, *14*, 1802−1805.
(40) Ma, Z.; Teo, A. J.; Tan, S. H.; Ai, Y.; Nguyen, N. T. Self-aligned interdigitated transducers for acoustofluidics. *Micromachines* **2016**, *7*, 216.
(41) Mikhaylov, R.; Wu, F.; Wang, H.; Clayton, A.; Sun, C.; Xie, Z.; Liang, D.; Dong, Y.; Yuan, F.; Moschou, D.; Wu, Z.; Shen, M. H.; Yang, J.; Fu, Y.; Yang, Z.; Burton, C.; Errington, R. J.; Wiltshire, M.; Yang, X. Development and characterisation of acoustofluidic devices using detachable electrodes made from PCB. *Lab Chip* **2020**, *20*, 1807−1814.
(42) Mikhaylov, R.; Martin, M. S.; Dumcius, P.; Wang, H.; Wu, F.; Zhang, X.; Akhimien, V.; Sun, C.; Clayton, A.; Fu, Y.; Ye, L.; Dong, Z.; Wu, Z.; Yang, X. A reconfigurable and portable acoustofluidic system based on flexible printed circuit board for the manipulation of microspheres. *J. Micromech. Microeng.* **2021**, *31*, 074003.
(43) Li, L.; Kong, W.; Chen, F. Femtosecond laser-inscribed optical waveguides in dielectric crystals: a concise review and recent advances. *Adv. Photonics* **2022**, *4*, 024002.
(44) Xu, B. B.; Zhang, Y. L.; Xia, H.; Dong, W. F.; Ding, H.; Sun, H. B. Fabrication and multifunction integration of microfluidic chips by femtosecond laser direct writing. *Lab Chip* **2013**, *13*, 1677−1690.
(45) Roth, G. L.; Esen, C.; Hellmann, R. Femtosecond laser direct generation of 3D-microfluidic channels inside bulk PMMA. *Opt. Express* **2017**, *25*, 18442−18450.
(46) Hayden, C. J.; Dalton, C. Direct patterning of microelectrode arrays using femtosecond laser micromachining. *Appl. Surf. Sci.* **2010**, *256*, 3761−3766.
(47) Zhang, Y. L.; Chen, Q. D.; Xia, H.; Sun, H. B. Designable 3D nanofabrication by femtosecond laser direct writing. *Nano Today* **2010**, *5*, 435−448.
(48) Ali, B.; Litvinyuk, I. V.; Rybachuk, M. Femtosecond laser micromachining of diamond: current research status, applications and challenges. *Carbon* **2021**, *179*, 209−226.
(49) Wang, X.; Yu, H.; Li, P.; Zhang, Y.; Wen, Y.; Qiu, Y.; Liu, Z.; Li, Y.; Liu, L. Femtosecond laser-based processing methods and their applications in optical device manufacturing: a review. *Opt. Laser Technol.* **2021**, *135*, 106687.
(50) Fu, Y. Q.; Luo, J. K.; Nguyen, N. T.; Walton, A. J.; Flewitt, A. J.; Zu, X. T.; Li, Y.; McHale, G.; Matthews, A.; Iborra, E.; Du, H.; Milne, W. I. Advances in piezoelectric thin films for acoustic biosensors, acoustofluidics and lab-on-chip applications. *Prog. Mater. Sci.* **2017**, *89*, 31−91.
(51) Zhang, Q.; Wang, Y.; Tao, R.; Torun, H.; Xie, J.; Li, Y.; Fu, C.; Luo, J.; Wu, Q.; Ng, W. P.; Binns, R.; Fu, Y. Q. Flexible ZnO thin film acoustic wave device for gas flow rate measurement. *J. Micromech. Microeng.* **2020**, *30*, 095010.

https://doi.org/10.1021/acsomega.2c07589
ACS Omega 2023, 8, 7838−7844